

Bio-Evaluation, *In-Vitro* and *In-Vivo* Anti-Inflammatory Activity, Therapeutic Efficacy, and Genotoxicity of the Potentials of the Green Seaweed *Valoniopsis Pachynema* using Zebra Fish Larvae (*Danio Rerio*) as an Animal Model

Bhuvaneshwari. J¹, Thirumalai Vasan. P^{2,*}

Bhuvaneshwari. J¹, Thirumalai Vasan. P^{2,*}

¹Research Scholar and adjunct faculty, Department of Biotechnology, Srimad Andavan College of Arts and Science (Autonomous), Affiliated to Bharathidasan University, Thiruvanaikovil, Tiruchirappalli, Tamil Nadu, INDIA.

E-mail: bhuvanaj2008@gmail.com

Orcid id: <https://orcid.org/0000-0002-1872-6913>

²Professor and Head, Department of Biotechnology, Srimad Andavan College of Arts and Science (Autonomous), Affiliated to Bharathidasan University, Thiruvanaikovil, Tiruchirappalli, Tamil Nadu, INDIA.

Orcid id: <https://orcid.org/0000-0001-8935-0389>

Correspondence

Thirumalai Vasan. P

Professor and Head, Department of Biotechnology, Srimad Andavan College of Arts and Science (Autonomous), Affiliated to Bharathidasan University, Thiruvanaikovil, Tiruchirappalli, Tamil Nadu, INDIA.

E-mail: thirubiotech@gmail.com

History

- Submission Date: 06-11-2022;
- Review completed: 09-12-2022;
- Accepted Date: 12-12-2022.

DOI : 10.5530/pj.2022.14.208

Article Available online

<http://www.phcogj.com/v14/6>

Copyright

© 2022 Phcogj.Com. This is an open-access article distributed under the terms of the Creative Commons Attribution 4.0 International license.

ABSTRACT

Advancement in the medical sectors to treat regular diseases are increasing day-by-day. Yet, there is a considerable growth in the demand for the natural/herbal products as well due to their low level of side effects, cost efficiency and their multiple inhibition properties. Based on this, the present research works with an objective to examine the bioactive components, *in vitro* anti-inflammatory and *in vivo* anti-inflammatory behaviour of the green marine macro algae *Valoniopsis pachynema* using zebra fish (*Danio rerio*) larvae as a skin inflammation model. In this study, the secondary metabolites are extracted using methanol solvent from the marine green seaweed, *V. pachynema* using the Gas Chromatography-Mass Spectrometry (GC-MS) analysis and these are further evaluated for their anti-inflammatory effects. Further screening process is accomplished for the *in vitro* anti-inflammatory activity by the albumin-denaturation inhibition. Results from concentration-dependent analysis is documented. The efficacy, therapeutic efficacy, and genotoxicity of the compound Valp at various concentrations are determined by recapitulating the pathophysiology of Skin inflammation in Zebrafish larvae. In evaluating the efficiency of the study, Valp at 1 pg, 10 pg, 100 pg are observed and progressed for the evaluation of therapeutic efficacy and genotoxicity. In the assessment of genotoxicity, the gene expression of mgmt gene is observed to be in control level at Valp 100 pg treated group confirming no genotoxicity. According to the results obtained, the green seaweed *V. pachynema* can be potentially explored as an effectual anti-inflammatory agent for its bio-functionalities.

Key words: *V. pachynema*, Marine algae, Bioactive compounds, Anti-inflammatory, GC-MS, Zebra fish larvae drug toxicity.

INTRODUCTION

In majority of therapeutic specialties, the concept of auto-immune and auto inflammatory illnesses is just beginning to gain ground, but it is especially relevant to the study of human dermatology.¹ A major component of the host's defense against many harmful agents, such as the invasion of foreign pathogens, physical injury, and other hostile immunological reactions, is regarded to be inflammation in general.^{2,3} However, persistent, arthritis, rheumatoid, asthma, multiple sclerosis, inflammatory bowel disease, diabetes, cancer and psoriasis are only a few of the disorders that can be triggered by excessive or protracted inflammation.⁴ Among these diseases, Psoriasis is one of the most frequent non-pathogenic skin conditions that have been identified so far. Psoriasis is a complex and multifaceted chronic inflammatory skin disease brought on by a confluence of hereditary and environmental factors.⁵ About 2-3% of the inhabitants worldwide have psoriasis. Psoriasis is characterised by telangiectasia in the dermal papillae, hyperproliferation of keratinocytes, and recruitment of inflammatory cells to the epidermis.⁶ Psoriasis is said to be caused because of the traumatic, environmental, or pharmacological stimuli that cause abnormal interaction among keratinocytes and various types of immune cell,

results in exposed increase of pro-proliferative and inflammatory circuits in susceptible individuals. Certain clinical symptoms associated with this disorder are plaque, psoriasis, inverse psoriasis, Psoriasis vulgaris, palmoplantar psoriasis, erythrodermic psoriasis, pustular psoriasis and scalp psoriasis.⁷⁻¹⁰

The entire skin surface of the body can also be affected.¹¹ Normal skin has a 30-day life cycle, but psoriasis has a 1.5–3-day life cycle. Nails and skin are frequently affected by psoriasis. Patients with psoriasis may also have concomitant conditions such as obesity, psoriatic arthritis, diabetes, metabolic syndrome, and cardiovascular diseases.¹² Consequently, it is also referred to as a T-cell mediated autoimmune illness. Interleukins (ILs), tumour necrosis factor (TNF-), and interferon-(IFN-) levels of inflammatory cytokines increase modestly in systemic circulation, but mostly in the dermis. Vascular-Endothelial Growth-Factor (VEGF) is created by mast cells, keratinocytes, and macrophages as a result of elevated levels of cytokines and other inflammatory mediators. New blood vessels are created as a result, increasing blood flow. According to recent research, there are 25 genetic variations that cause psoriasis. The cause of psoriasis is immune system activation, and the psoriasis-causing gene has been found. This could give precise and effective treatments to treat psoriasis.¹³

Cite this article: Bhuvaneshwari J, Vasan PT. Bio-Evaluation, *In-Vitro* and *In-Vivo* Anti-Inflammatory Activity, Therapeutic Efficacy, and Genotoxicity of the Potentials of the Green Seaweed *Valoniopsis Pachynema* using Zebra Fish Larvae (*Danio Rerio*) as an Animal Model. Pharmacogn J. 2022;14(6)Suppl: 1037-1053.

Recently, as there is huge scope for the anti-inflammatory agents, the investigators have recognised marine algae as a compound that is said to be rich in anti-inflammation.^{14,15} One of the marine entities that has been investigated the most is macroalgae. Biological effects such as antioxidant, anticancer, antihypertension, hepatoprotective, immunomodulatory, and neuroprotective actions have been documented in earlier investigations.^{16,17} Along with polysaccharides, proteins, lipids (PUFA, sterols, and squalene), minerals, and vitamins, macroalgae are also known to include secondary metabolites such as phenolic compounds, terpenoids, and halogenated chemicals that are connected with protection against UV radiation.¹⁸ The green seaweed *Valoniopsis pachynema* is rich in carbohydrates, proteins and other macro nutrients such as sodium, potassium, phosphate and other vital minerals.^{19,20} India, Northern and Eastern Australia, Indonesia, the Philippines, the Gulf of California, the West Indies, Mauritius, Pakistan, East Africa, Sri Lanka, and Spain are some of the most habitually found locations for the green seaweed *Valoniopsis pachynema*.²¹ In India, the south-east coast is where *V. pachynema* is most prevalent from September to November.²² Until now, the only studies that have been conducted have predominantly focused on this seaweed's antioxidant abilities,²³ corrosion inhibition,²⁴ papermaking,²⁵ and biohydrogen production.²⁶ Nevertheless, there is still a dearth of scientific evidence on the detailed chemical and pharmacological profile of this green seaweed.²⁷ Hence, the ultimate goal of this current investigation is to fill in the literary gaps about the potentiality and the ameliorative effects of this seaweed in skin inflammation.²⁸

The use of an *in vivo* approach makes it easier to understand how various medications, chemicals, and known environmental contaminants affect animals, not only at the cellular and tissue levels but also with regard to the intricate metabolic processes occurring across the animal's many tissues. Innumerable studies on genotoxicity have been conducted using mice^{29,30} and rats.^{31,32} However, since many animals must be used and a lot of test substances have to be employed, *in vivo* models wind up being highly expensive. It can take up to two years to ascertain whether a substance is cardiotoxic in rodents. Since invasive methods will be used to evaluate different drug effects, the process is time-consuming, and the models are unfeasible for high-throughput screening. Furthermore, the use of mammalian models in toxicity studies is complicated by legal and moral concerns.³³

In contrast, zebrafish is a cost efficient and coherent vertebrate model, which is a very appealing alternative because of its distinguished physiological and genetic homology to humans.³⁴ It possesses a quick generation period, well-defined rapid developmental stages, and is acquiescent to gene manipulation. The whole-body plan is developed during the first 24 hours following fertilization, and the structural layout and organ systems are extremely similar to those of other vertebrates, including humans.³⁵ Zebrafish are quintessential models for examining the effects of chemical compounds on healthy development and illness with the highest temporal efficiency. It has a very low maintenance cost and can be bred in considerable quantities. It just takes a minimal quantity of drugs or other chemical substances to conduct the test since the larvae are so small and susceptible to medications. As a result, zebrafish larvae are the most economical *in vivo* drug screening model and can be used for high-throughput assays.^{36,37}

Inflammation determination,³⁸ chemical screening,^{39,40} microarrays and proteomic studies⁴¹ have all made use of high-throughput experiments. The transparent nature of the larvae makes them ideal for *in vivo* imaging without the need for any intrusive procedures.⁴²⁻⁴⁶ Therefore, the present study aims in identifying the bio-active components, *in vitro* anti-inflammatory and *in vivo* anti-inflammatory capacities of green marine macro algae *V. pachynema* for this the study chosen transgenic zebra fish as an animal model. The exploration also evaluated the bio-active components of the green marine macro algae *V. pachynema* using Gas Chromatography-Mass Spectrometry (GC-MS) techniques.

The present research work is undertaken to encompass the following objectives:

To identify the bioactive components, *in-vitro* anti-inflammatory and *in-vivo* anti-inflammatory capacities of green marine macro algae *V. pachynema* using GC-MS technique for analysing the potential inhibitory effects against clinical enzymes which are associated with the chronic skin inflammation.

To assess the therapeutic efficacy, genotoxicity of the extracted concentrations of the green marine macro algae thereby to study the pathophysiology of skin inflammation in a transgenic zebra fish animal model.

To examine the efficiency of the present study, the research data is analysed and correlated by utilizing multivariate analysis.

Paper organization

In section 1, the brief introduction and objective of the present research work is deliberated. Followed by this, the materials and methods utilized in the present investigation is discussed in section 2. Section 3 clearly represents the results obtained from the proposed study and the paper is concluded in the section 4.

MATERIALS AND METHODS

The materials and the methods followed in the study for the exploration are deliberated in this section.

Collection of algae

In order to carry out the methodology of the proposed study, the marine green macro algae *Valoniopsis pachynema* was fetched from the internal shallow zone of the Mandapam area, in Ramanathapuram district. The collected algae were extracted from the coast of Mandapam, Rameshwaram located in the east-coastal regions of Tamil Nadu. The collected algae were cleansed with water to separate it from the epiphytes and sand. Later, it was stuffed in a polythene cover and was taken to the lab for further investigation. The obtained algae were rinsed with the distilled water to completely remove the marks of the sand and other contaminations, dried in the shade and stored appropriately for later study.

Validation of algae

The algae that was obtained as depicted in the previous section was examined by Dr. V. Veeragurunathan, senior scientist, CSIR- Central Marine Algal Research station, in Mandapam, Ramanathapuram district, Tamil Nadu in India. The obtained algae that is recognised as *Valoniopsis pachynema* was employed for the examination process.

Research of crude extract from marine algae

The green seaweed *V. pachynema* was dried in the shade for around 10 days. The dried seaweed was powdered in the commercial grinder. Seaweed sample was also powdered, stored and weighed. Direct extraction technique using methanol as a solvent was used in the preparation of the algal extract to yield a good quality extract. The obtained extract was then left to settle for 24 hours at room-temperature and stirred regularly. After the time period of 24 hours, the sample was filtered with the What-man filter paper. Some unnecessary filtrates were detached through the filtration mechanism and then the extraction was kept under the refrigerator temperature until next research process.

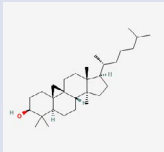
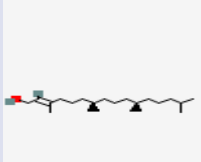

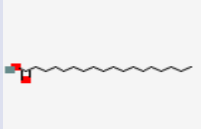
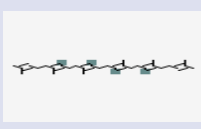
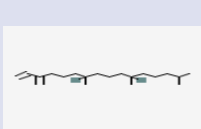
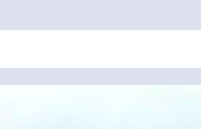
GC-MS analysis

The assessment of bioactive mixtures from the methanol extraction of the green seaweed *Valoniopsis pachynema* disclosed the existence of bioactive mixtures. Results of GC-MS paved to the recognition of

Table 1: Natural volatile components identified in the methanolic extract of the green marine algae *valoniopsis pachynema*.

Peak	Constituents	R. Time	Peak Area
1	Octadecane	8.912	0.53
2	Cycloartanol	9.284	0.62
3	Bromoacetic acid, 3-pentadecyl ester	9.506	0.58
4	10-Heptadecen-8-ynoic acid methyl ester, (E)	9.766	0.60
5	6-O-Methyl-2,4-methylene-beta -sedohepitol	10.119	0.76
6	N.alpha.-[N-(tert- butoxycarbonyl)methylonyl	10.149	0.78
7	Curan-19,20-diol	10.320	0.58
8	1-Ethyl-3,cis-(1,1-dimethylethyl)-4	10.476	0.61
9	5-Chloro-2-nitrocinnamic acid	10.890	0.62
10	Pseudoarsasapogenin-5, 20-dien methyl ester	11.051	1.24
11	7-Hydroxy-3-(1,1-dimethylprop-2-enyl) coumarin	11.136	0.53
12	2(1H)-Naphthalenone	11.174	0.65
13	2(2'-Phenyl-3'-oxo-butyl)-cyclopentanone	11.237	0.62
14	(3R,3aR,7R,8aS)-3,8,8-Trimethyl-6-methyleneoctahydro-1H-3a	11.367	0.53
15	Cycloheptasiloxane	12.453	0.57
16	Pentadecane	12.960	0.64
17	2,4-Di-tert-butylphenol	13.100	0.56
18	Cyclooctasiloxane	14.519	1.07
19	Eicosane	15.451	0.65
20	Tetradecanoic acid	16.168	5.75
21	Cyclononasiloxane	16.326	0.97
22	Neophytadiene	17.017	2.62
23	2-Pentadecanone	17.084	2.69
24	Neophytadiene	17.286	1.36
25	Neophytadiene	17.488	1.18
26	7,9-Di-tert-butyl-1-oxaspiro(4,5)deca	17.826	0.79
27	Cyclodecasiloxane	17.926	0.73
28	Hexadecanoic acid, methyl ester	17.978	3.03
29	l-(+)-Ascorbic acid 2,6-dihexadecanoate	18.362	21.38
30	1,3-Diisopropoxy-1,3-dimethyl-1,3-di	18.513	1.93
31	Cyclononasiloxane, octadecamethyl-	18.640	1.57
32	Silane, chlorodiethylheptyloxy-	18.686	0.53
33	Bromoacetic acid, octadecyl ester	18.777	1.54
34	Cyclononasiloxane	19.375	0.64
35	Phytol	19.871	6.37
36	Methyl stearate	20.016	0.89
37	cis-13-Eicosenoic acid	20.186	2.55
38	Docosanoic acid, isopropyl ester	20.282	1.03
39	Octadecanoic acid	20.372	1.21
40	Methyl (1R,2R,8aS)-2-(methoxycarbonyl)-2-hydroxy-5	20.459	0.60
41	Tetradecanamide	20.560	0.79
42	Cyclononasiloxane	20.685	0.97
43	Glycidyl palmitate	21.612	1.28
44	Cyclononasiloxane, octadecamethyl	21.904	0.97
45	Cyclononasiloxane	23.044	0.73
46	6.beta.-Hydroxymethandienone	23.374	0.54
47	Diisooctyl phthalate	23.654	1.09
48	Beta.-Tocopherol	23.826	0.76
49	Codeine-propionyl	24.019	1.07
50	1,4-Bis(methylsulfinyl)piperazine	24.041	0.83
51	Cyclononasiloxane, octadecamethyl	24.112	1.07
52	Glutaric acid, dodecyl 2-nitrobenzyl ester	24.162	0.62
53	18,19-Secolupan-3-ol	24.274	0.64
54	1,2,4-Triazol-3-amine	24.973	1.49
55	Cyclononasiloxane, octadecamethyl	25.127	0.93
56	N-(6-Acetamido-1,3-benzothiazol-2-yl) acetamide	25.154	0.54
57	(2R,3R,4aR,5S,8aS)-2-Hydroxy-4a, 1(2H)-Naphthalenone	25.284	0.60
58	2,6-Lutidine 3, 5-dichloro-4-dodecylthio	25.567	1.20
59	Tetracosamethyl-cyclododecasiloxane	25.704	6.65
60	Tetrahydropyran-4-carboxylic acid,	25.774	0.97
61	Squalene	25.843	4.19

Table 2: A few major 7 compounds identified in the methanolic extract of the green seaweed *valoniopsis pachynema*. *In vitro* anti-inflammatory activity

COMPOUND	MOLECULAR FORMULA	PUB CHEM CID/ CAS	IUPAC NAME	CLASS OF COMPOUNDS	MOLECULAR STRUCTURE
Cycloartanol	C ₃₀ H ₅₂ O	4657-58-3	(1S,3R,6S,8R,11S,12S,15R,16R)-7,7,12,16-tetramethyl-15-[(2R)-6-methylheptan-2-yl]pentacyclo[9.7.0.0 ^{1,3} .0 ^{3,8} .0 ^{12,16}]octadecan-6-ol	Sterol Lipids	
Eicosane	C ₂₀ H ₄₂	528491	Icosane	Alkanes	
Phytol	C ₂₀ H ₄₀ O	5280435	(E,7R,11R)-3,7,11,15-tetramethylhexadec-2-en-1-ol	Acyclic diterpenoids	
Cis-13 Eicosenoic acid	C ₂₀ H ₃₈ O ₂	5312518	(Z)-icos-13-enoic acid	Long-chain fatty acids	
Octadecanoic acid	C ₁₈ H ₃₆ O ₂	5281	Octadecanoic acid	Long-chain fatty acids	
Squalene	C ₃₀ H ₅₀	638072	(6E,10E,14E,18E)-2,6,10,15,19,23-hexamethyltetracos-2,6,10,14,18,22-hexaene	Triterpenoids	
Neophytadiene	C ₂₀ H ₃₈	10446	7,11,15-trimethyl-3-methylidenehexadec-1-ene	Sesquiterpenoids	

various kinds of bio-active mixtures found in the extract, the recorded outcomes have been illustrated in the table 1 and 2. The structure of the compounds during the investigation were tested on the basis of the fragmentation arrangement of the mass spectra. The structure was also compared directly with published mass spectra as well as their chemical outlines found in the NIST (National institutes of standards and technology) library, Gaithersburg, Md, D, USA. The information regarding the chemical outlines with their retaining time, molecular formula, peak percentage area and identified structure of the mixtures are demonstrated in the table 1. Thus, the characterisation of the ethanol extract with the GCMS test confirmed the existence of other metabolic compounds that possess beneficial features like anti-inflammatory, antioxidant, antimicrobial, anticancer

In vitro anti-inflammatory activity

The process of albumin denaturation inhibition assay was carried out by the following the procedure provided by.⁴⁷ The mixture of the reaction has various concentration sample with the pH of the mixture and 1% of aqueous solution albumin fraction has been formulated with 1N HCl. The reaction of the extracted mixture was nurtured at 37 °C for 20 min later the mixture was warmed up at 51 °C for 20 min and set it to cool at normal room temperature. The absorbance of the compound was read at the wavelength of 660 nm with the spectrophotometer, aspirin was employed as standard and the activity was predicted through the formula that is demonstrated below equation (1).⁴⁸



Figure 1: Morphological features of the green marine macro algae *Valoniopsis pachynema*.

$$\text{Protein inhibition (\%)} = \frac{(\text{Abs Control} - \text{Abs Sample}) \times 100}{(\text{Abs Sample})} \quad (1)$$

In vivo anti-inflammatory activity

Zebra fish husbandry and maintenance

The strains of zebra fish (*Danio rerio*) used were AB wild type animals adapted and bred at Pentagrit research, Chennai. All fishes were

acclimated to constant laboratory condition (14-h light:10-h dark photoperiod, water temperature of 28 +/- 1 °C and pH between 6.8-7) in stock aquaria. Adult fish were fed Tetra fish flakes (A complete pet food for Tropical fish from Tetra GmbH, Herrenteich) daily, until the beginning of the experiment. The adult zebrafish including both males and females were conditioned for 2 weeks under laboratory husbandry conditions in stock aquaria prior to the study. Random adult male fishes were opted from different clutches for this experiment. Groups of 24 adult fishes were housed in transparent polycarbonate tanks. Good Animal Practice as per Institutional Animal Ethics Committee in accordance with Committee for the Purpose of Control and Supervision of Experiments (CPCSEA), India, were followed in adherence to established protocols. Housing tanks were cleaned once in 4 days to keep the fishes clean and free from infection.

Mode of induction

The forward genetic method as per⁴⁹ was employed. Adult Zebra fish males were subjected to the ENU chemical mutagen to induce random mutagenesis, administered through water dissolution method. Prior to the spawning, the induced male zebra fish, and adult females (herein referred to as Zebrafish founders) were housed separately under standard laboratory husbandry circumstances were set for spawning at a spawning ratio of female to male fish 1:4 per breeding tank. The generated pool of F1 mutants were screened for presence of epidermal aggregates,⁵⁰ loss of function mutations in CARD14 are associated with severe variant of atopic dermatitis. The F1 mutants carrying CARD14 mutation were inbred and the resulting F2 embryos (henceforth addressed as CARD14) were employed for the study purpose. Sperm from CARD14 fish were collected and cryopreserved following methods as per⁵¹ to recover CARD14 fish as per experimental necessity.

The CARD14 embryos were housed and maintained in embryo medium. Quality check of the embryonic development was done using LaboMed LX400 brightfield microscope with Labomed Camera LC-5 1080P C-MOUNT WIFI CMOS. The embryos displaying an opaque discoloration were repudiated and only the embryos with best growth phase were chosen for the study purpose. The chosen embryos were transferred to a four-litter housing water and were housed in a ratio of 250 per housing tank of 25 liters' capacity thereby providing adequate space for swimming motion and minimizing the factor of crowding. CARD14 model screening was carried out for two days from the day of hatching, and the larvae (3dpf- 4 dpf) demonstrating the epidermal

aggregates were advanced for dosing purpose. During the larvae developmental stages (3 dpf- 4 dpf), the study tanks were conditioned (under a water temperature of 28 +/- 1 °C and pH between 6.8-7.5) and were incessantly examined for mortality and Phenotypic changes. The overall Experimental Scheme for the Evaluation of Toxicity of the Green Seaweed *Valoniopsis Pachynema* is shown in figure 2.

Measurement of toxicity of the crude extract compound

Efficacy screening

Group setting was done for the following classes- Treated groups, Model, and control, and a distribution pattern of 24 larvae per group and 6 larvae per 30 ml of embryo medium were housed. The Valp compound with varying dilution was administered by means of water dissolution dosing during day 1 (5dpf), day 3 (7dpf), day 5 (9 dpf), day 7 (11 dpf) at calculated dosing volumes. Constant monitoring of the reduction in epidermal aggregates and a 48h washout cycle was conducted for larvae. On day 7, post 2 hours of dosing, screening was carried out for all the study groups to determine the efficacy of the Valp compound. The concentration of Valp that showed reduction in epidermal aggregated and better survival rate were selected and advanced for investigating therapeutic activity and genotoxicity.

Drug screening and genotoxicity

Group setting was done for the following classes- Treated groups, Model, and control, and a distribution pattern of 60 larvae per group and 6 larvae per 30 ml of embryo medium were housed. The Valp at concentrations that were selected from efficacy screening and Methotrexate at 0.54 pg were administered through water dissolution during day 1 (5dpf), day 3 (7dpf), day 5 (9 dpf), day 7 (11 dpf). On day 7, post 2 hours dosing screening was carried out for all the study groups to determine the therapeutic activity and genotoxicity of the Valp compound. For efficacy and drug screening the compound at various dilutions were dosed by means of water dissolution method. The compound was completely soluble in distilled water. The logarithmic dose of 1 pg, 10 pg, 1 ng, 10 ng, 100 ng were adopted for water dissolution dosing. Further dilutions were prepared from the stock; desired doses were derived for a 10µl of water dissolution volume. The volume of the compound for water dissolution was escalated 10 times to that of the desired dose for 30 ml of water to ensure the bioavailability of the compound for each larvae.

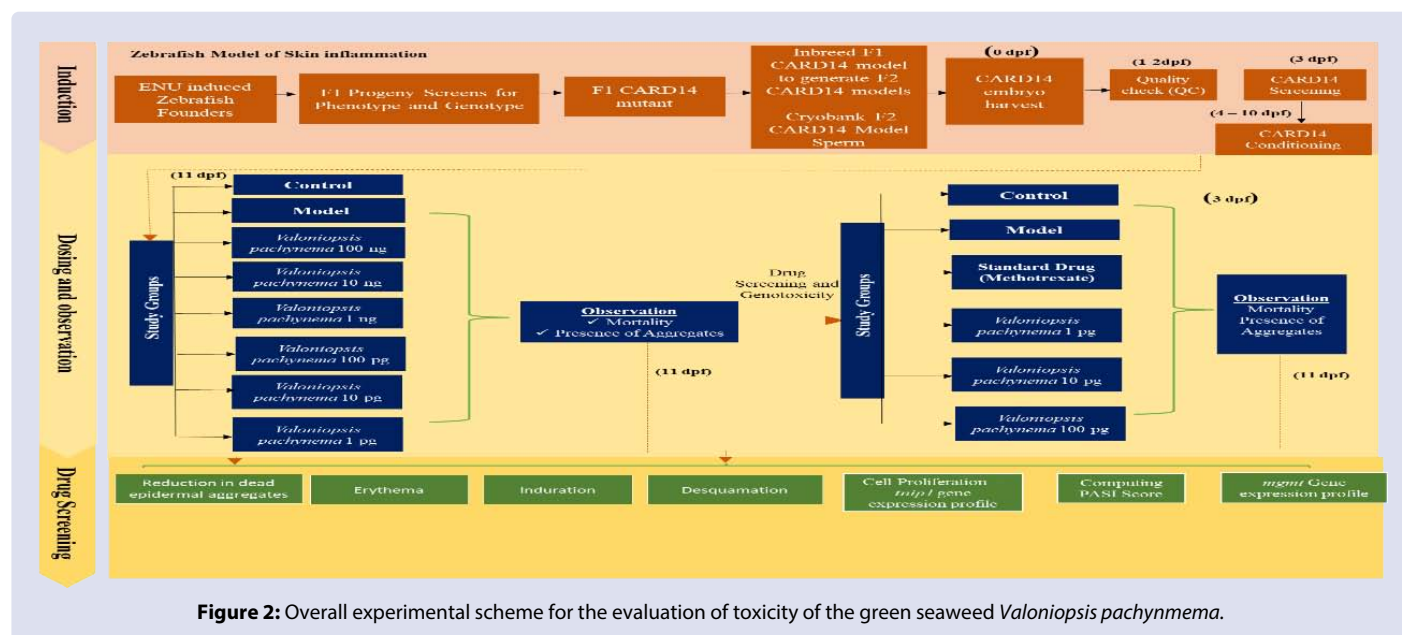


Figure 2: Overall experimental scheme for the evaluation of toxicity of the green seaweed *Valoniopsis pachynema*.

Zebrafish larvae maintenance post dosing

Post dosing, the 5 dpf larvae were carefully monitored for alterations in the presence of epidermal aggregates for a period of 7 days. Proper care was taken, and the larvae were housed at temperature (25 +/- 1 °C) to aid the physiological changes. A 48h washout cycle was precisely followed to eliminate the probability of mortality and improve the survival odds. As the dosage was unknown, the logarithmic dose of 1 pg, 10 pg, 100 pg, 1 ng, 10 ng, 100 ng were adopted for efficacy screening for treated groups to determine the efficacy dose concentration by monitoring the reduction in dead epidermal aggregates. Further the selected dose was advanced for evaluating therapeutic efficacy and genotoxicity of the compound.

Screening assays for drug toxicity

Assay 1: Reduction in dead epidermal aggregates

Skin inflammation model display dead epidermal aggregations, showing the possibility that the skin inflammation is due to perturbations in the integrity of the epidermal cells.⁵⁰ To study the reduction in epidermal aggregates zebrafish larvae were anesthetized with 0.03% Tricaine (Sigma-Aldrich) solution for 1min. A reduction in the reflex and locomotor activity upon stimulus were noted in the anaesthetic zebrafish larvae. Post sedation, the larvae was gently mounted on Glass slide covered with minimal water. Imaging: Prepared slides were observed under 40X magnification using Labomed LX 400 Light microscope. Images were captured using Labomed Camera installed with the Imageview Interface. The reduction in epidermal aggregates were manually calculated from the obtained images.

Assay 2: Erythema- distribution of redness in pixel intensity

Skin inflammation model at severe stage exhibits erythema. Erythema herein referred to distribution of red pixels in the extremities of the zebrafish larvae. The images were used further to measure the intensity of the redness present in the skin of zebrafish larvae. The raw image files were processed using Image J software with histogram analysis. The data obtained were further analyzed for red pixel distribution across the area of interest. Sum and standard deviation were computed for statistical representation of data.

Assay 3: Induration – measures of thickness of aggregates

The thickness of the epidermal aggregates was measured using the acquired images. The raw image files were processed using Image J software with histogram analysis. Histogram analysis is used to measure the intensity of the region of interest. The presence of epidermal aggregate was observed to have reduced intensity. The standardization of histogram analysis was done using a control larva where the region of evenly distributed cells showed higher pixels and aggregates were noted to have reduction in number of pixels. The pixels obtained from the histogram analysis were converted to mm scale by known pixels per mm.

Assay 4: Desquamation- measures of descaling on the epidermis

The skin inflammation model at severe stage exhibits desquamation of the cells. The raw images were processed using Image J software with the measure analysis tool to measure the area of desquamation. The sum and standard deviation of the area obtained from the analysis were computed for statistical representation of data.

Assay 5: Cell proliferation - expression profile of *tnip1* gene by semi quantitative RT PCR

The *tnip1* gene that encodes NF- α -induced protein 3-interacting protein 1 is a strongly linked to susceptibility of psoriasis.⁵² Downregulation

of *tnip1* gene leads to increase in proliferation of keratinocyte that is observed in severe type of psoriasis. Here the gene expression of *tnip1* gene was evaluated through semiquantitative RT PCR method.

Assay 6: Adopted PASI score

The PASI score is evaluation of the severity of erythema, induration, desquamation, and the area of the body involved. PASI score is employed for the assessment the severity of psoriasis. Here the PASI score is predicted using the score of erythema, in-duration, desquamation, and the area of the body involved for zebrafish larvae. In the present study the PASI score was adopted from Human PASI score.

Gene expression analysis

The evaluation of Gene expression is discussed in this section;

Expression profile of *mgmt* gene by semi quantitative RT PCR sample collection

The fry is sedated with ice cubes for 2-3minutes for rapid cooling euthanization. The samples of 30 larvae were harvested and stored together in 150 μ l acid phenol at -20° C until RNA extraction.

RNA extraction

The total RNA was extracted with the help of the phenol-chloroform extraction technique as deliberated by.⁵³ The method is based on phase separation of the sample and aids in the isolation of desired RNA. The sample was homogenized in 300 μ l of Acid phenol. A volume of 250 μ l of chloroform was added to the homogenate and vortexed for few seconds. The sample was incubated in the ice bath for 15 mins. After incubation, the sample was vortexed at high speed for 1 minute followed by centrifuge at high speed for 10 mins. This yielded three distinct phases as follows – clear aqueous phase containing RNA, thin interphase containing cellular debris and lower phase with organic substances. The aqueous phase containing RNA was transferred to a fresh centrifuge, and 100 μ l of isopropanol was added to the tube followed by incubation in ice bath for 40 mins. At the end of ice incubation, the sample was centrifuged at full speed for 10 mins to precipitate RNA. The supernatant was discarded and the tube containing RNA pellet was dried in the incubator at 40° C to evaporate isopropanol. The RNA quality was evaluated with gel electrophoresis and the aliquots were directly used for reverse transcriptase reaction. Reverse Transcriptase cDNA was synthesized from total RNA (20 μ l final reaction volume) with oligo(dT) 15 primer using AMV reverse transcriptase (First strand cDNA synthesis kit; Roche) according to manufacturer's instruction. The cDNA tubes were stored at -20° C until use.

To study the gene expression, *mgmt* gene was used. 18s RNA was selected as control gene. Since most of the usually employed study genes have been said to be different from under experimental conditions, for quantifying the gene expression changes in Zebrafish, the internal control gene (18s RNA) that stably expressed under different experimental conditions was used to normalize the study gene.⁵⁴ All the primers used in the study were designed using NCBI primer blast tool. The primers were synthesized from Sigma Aldrich and the following primers listed below was used for the study assessment.

PCR amplification

PCR amplification was performed using the cDNA as template with a reaction volume of 20 μ l as mentioned in Table 4 and the PCR conditions were set as 94°C for 2 mins, 95°C for 5 mins and 72°C for 5 mins tabulated in Table 6. All the qPCR reactions were performed in triplicates and the negative control did not contain any sample template. At the end of 30 cycles, a 6 μ l aliquot of each sample was mixed with 2.5 μ l of gel loading buffer and electrophoresed on an agarose gel for 15 mins. The gel was observed under the UV transilluminator for

Table 3: Reduction in dead epidermal of aggregates.

Study Groups	Number of Aggregates	SD
Control	0	0.00
Model	6	1.04
Valp 1 pg	2	1.89
Valp 10 pg	2	0.76
Valp 100 pg	3	0.86
Valp 1 ng	5	2.10
Valp 10 ng	6	0.91
Valp 1 ng	6	1.96

Table 4: Survival rate.

Study Groups	Survival Percentage
Control	100
Model	92
Valp 1 pg	83
Valp 10 pg	83
Valp 100 pg	92
Valp 1 ng	100
Valp 10 ng	83
Valp 100 ng	83

Table 5: Reduction in dead epidermal of aggregates.

Study Groups	Number of Aggregates	SD
Control	0.0	0.00
Model	5.1	2.59
Methotrexate	3.3	1.25
Valp 1 pg	4.2	1.07
Valp 10 pg	2.8	0.69
Valp 100 pg	2.5	0.50

Table 6: Erythema – distribution of redness in pixel intensity.

Study Groups	No. of Pixels with Redness	SD
Control	0	0
Model	76	5.27
Methotrexate	65	11.26
Valp 1 pg	32	11.24
Valp 10 pg	21	0.67
Valp 100 pg	19	9.47

bands. A 1 µl aliquot of the tester was diluted in 2 ml distilled-water and used for UV spectroscopy under 260 nm absorbance to determine the concentration of the DNA.

Statistical analysis

For statistics data, one-way ANOVA was used by GraphPad Prism 8.0 software and all data were displayed graphically as the mean and standard deviation of means and $P < 0.05$ considered significant. Analysis of the mean was carried out by One Way ANOVA test with post-hoc Tukey's test to estimate significance of the data.

RESULTS AND DISCUSSION

The result obtained with the implementation of above stated method are discussed in the followings;

Chemical composition of *V. Pachynema* methanolic extract

In the present study, an attempt has been made to investigate and study the presence of various chemical constituents, *in vitro* anti-

inflammatory and *in vivo* anti-inflammatory properties of the green seaweed, *V. pachynema*. GC-MS analysis of the crude methanolic green marine algal extract led to the identification of 61 compounds. It was found that the crude methanolic extract revealed the high peak intensity and the various predominant presence of major compounds like 1-(+)-Ascorbic acid 2,6-dihexadecanoate (21.38%), Tetracosamethylcyclohexadecasiloxane (6.65%), Phytol (6.37%), Tetradecanoic acid (5.75%), Squalene (4.19%), Hexadecanoic acid, methyl ester (3.03%), Neophytadiene (2.62%), and cis-13-Eicosenoic acid (2.55%) among other derivatives. Figure 3 shows the chromatogram of Green Algae.

Most biological proteins are denatured during the process of albumin denaturation, which results in the loss of their biological activity. Inflammation is thought to be brought on by protein denaturation. The anti-inflammatory effects of the *Valoniopsis pachynema* methanolic extraction have been examined by the inhibition of albumin denaturation activity. The results of the present research have depicted in figure 4 that the *Valoniopsis pachynema* methanolic extract has reflected high concentration based protein-denaturation effect with 80.39% at 500 µg/ml. Whereas the commercial drug was observed to reveal strong potential when compared to the *V. pachynema* extracts and the outcomes of the research revealed for 94.62% at similar level of concentration.

Mean ± SD (n = 3): The entire determinants were conceded out in triplicates. All the standards in the table 1 are evaluated to be statistically significant at $p < 0.05$. *In vitro* Anti-inflammatory activity of the crude methanolic extract of *V. pachynema* by Inhibition of albumin denaturation method is shown in figure 4.

Efficacy screening

Assay 1: Reduction in dead epidermal aggregates

The correlation result obtained in the efficacy screening are shown in this section. Figure 5 represents Zebrafish Larvae image at 40X magnification; (a) Control, (b) Model, (c) Valp 1 pg, (d) Valp 10 pg, (e) Valp 100 pg, (f) Valp 1 ng, (g) Valp 10 ng, (h) Valp 100 ng and the table 3 shows the reduction in Dead Epidermal of Aggregates.

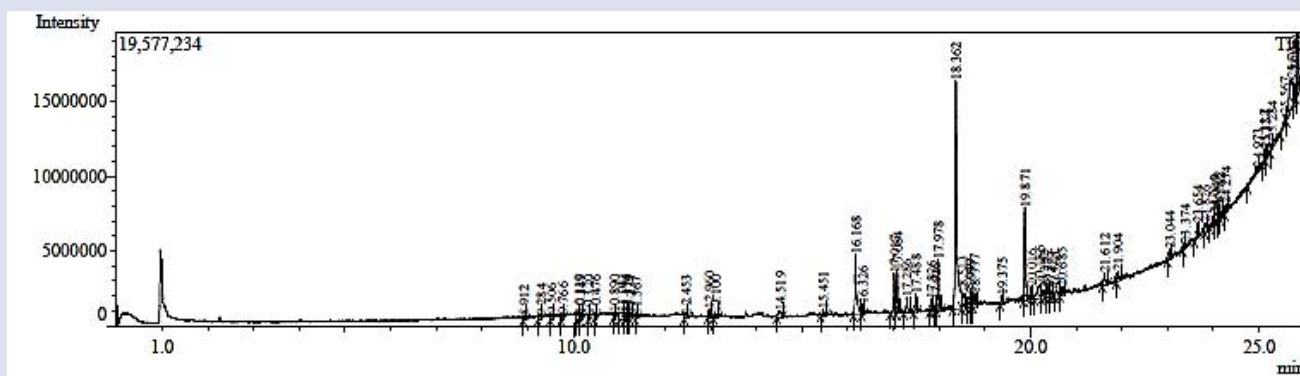
Figure 6 represents number of aggregates observed in the epidermis and extremities where the mean of model is compared to mean of control. It has been observed that the control and model group revealed a significant difference in the numerous of dead epidermal aggregates. The model showed presence of epidermal aggregates in the extremities of the zebrafish larvae whereas control did not exhibit dead epidermal aggregates. A comparatively higher number of epidermal aggregates was noted in model which demarcates the presence inflammatory suppression thereby leading to the formation of epidermal aggregates.

The mean of the model was compared to compound treated groups across various dilutions. Valp at 1 pg and 10 pg displayed a significant reduction in number of epidermal aggregates with a mean value of 2. Whereas at 100 pg a modest rescue in the numerous of aggregates has been evaluated with mean of 3 aggregates. Upon increasing the treated dilutions, Valp at 1 ng, 10 ng, 100 ng did not show significant reduction in epidermal aggregates indicating absence efficacy across the respective dilutions. Therefore, Valp at 1 pg, 10 pg, 100 pg were identified to have efficacy in rescuing the number of aggregates and were further used to evaluate for drug screening and genotoxicity assays.

Kaplan-Meier survival curve – efficacy screening

The Kaplan-Meier Survival Curve – efficiency screening result are shown in this section. Table 4 results the survival rate using Kaplan-Meier Survival Curves.

Figure 7 represents the Kaplan Meier survival curve of the larvae for efficacy screening. The WT showed a 100% survival rate and no mortality. Whereas model marked 92% survival with one mortality on day 7.



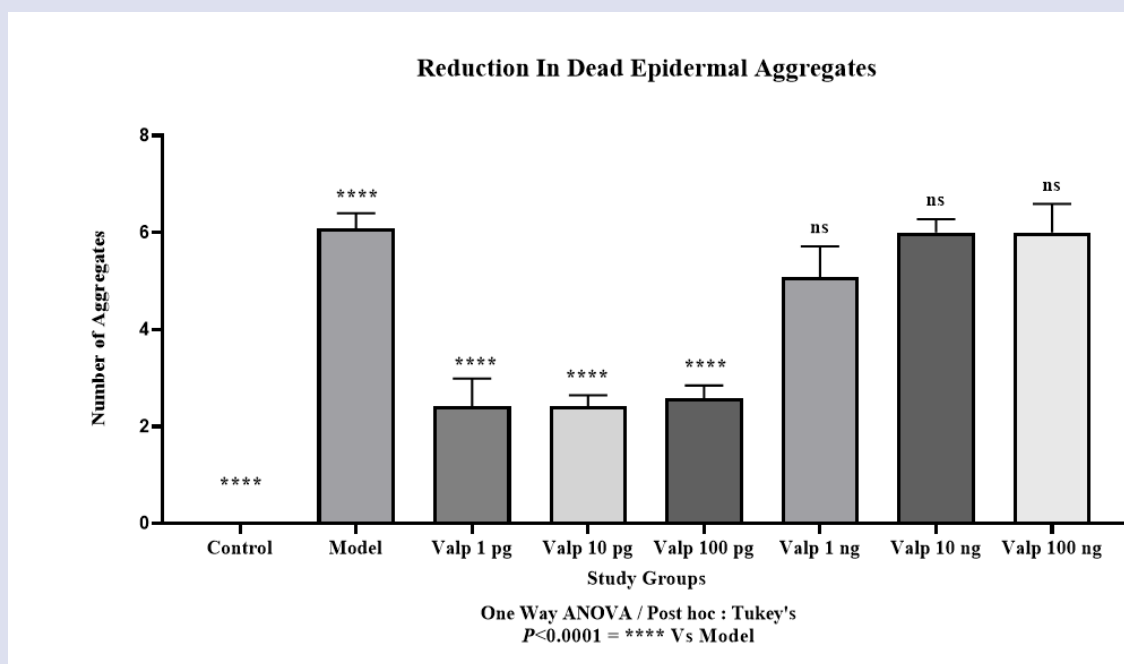


Figure 6: Reduction in dead epidermal aggregates.

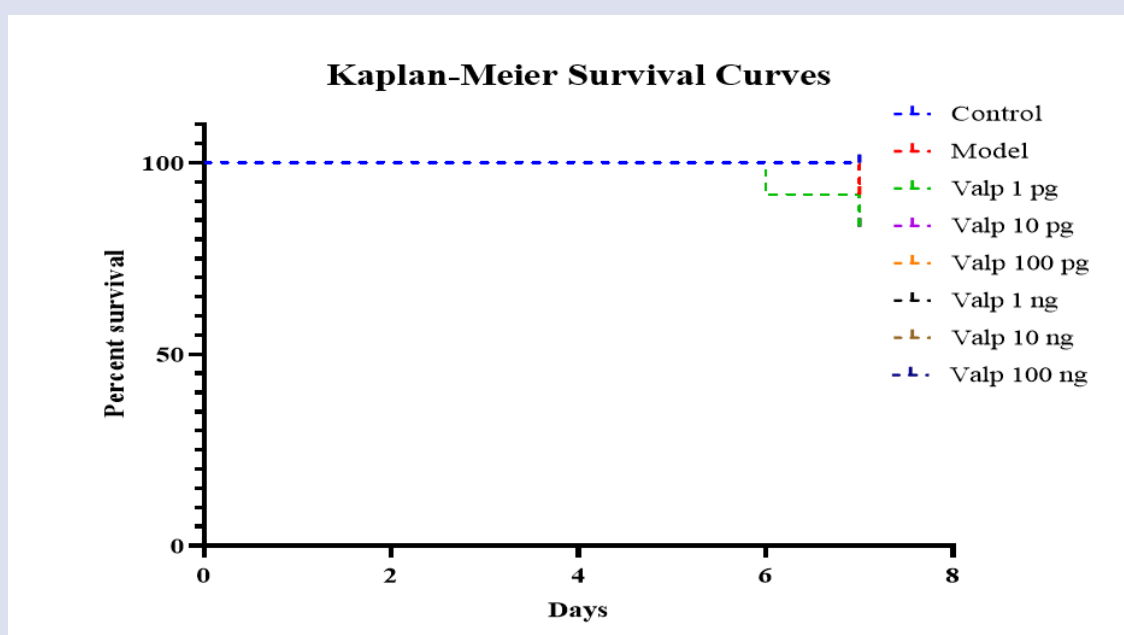


Figure 7: Represents Kaplan-Meier survival curve – efficacy screening.

The mortality of Valp treated group at 1 pg, 10 pg, 10 ng and 100 ng showed 83% survival rate. Valp at 100 pg showed improved survival rate with 92% survival. Valp at 1 ng did not show mortality throughout the study period.

Drug screening

Assay 1: Reduction in dead epidermal aggregates

The drug screening results are discussed in this section. Figure 8 shows the Zebrafish Larvae image at 40X magnification; (a) Control, (b) Model, (c) Methotrexate, (d) Valp 1 pg, (e) Valp 10 pg, (f) Valp 100 pg. Along with this, the table 5 shows the reduction in dead epidermal of aggregates.

Figure 9 represents the number of aggregates observed where the mean of model is compared to mean of control. Control and model showed significant difference in total number of dead epidermal aggregates. Model exhibited comparatively higher number of dead epidermal aggregates with mean of 5. The mean of model was compared to methotrexate treated group where a significant reduction in dead epidermal aggregates was observed with mean of 3 indicating moderate rescue.

The mean of model was compared to Valp treated group across various dilution. Valp at 1 pg did not show any significant reduction in dead epidermal aggregates indicating no rescue. Whereas Valp at 10 pg and 100 pg exhibited a significant reduction in dead epidermal aggregates confirming moderate rescue in reduction of dead epidermal aggregates.



Figure 8: Zebrafish larvae image at 40X magnification; (a) Control, (b) Model, (c) Methotrexate, (d) Valp 1 pg, (e) Valp 10 pg, (f) Valp 100 pg.

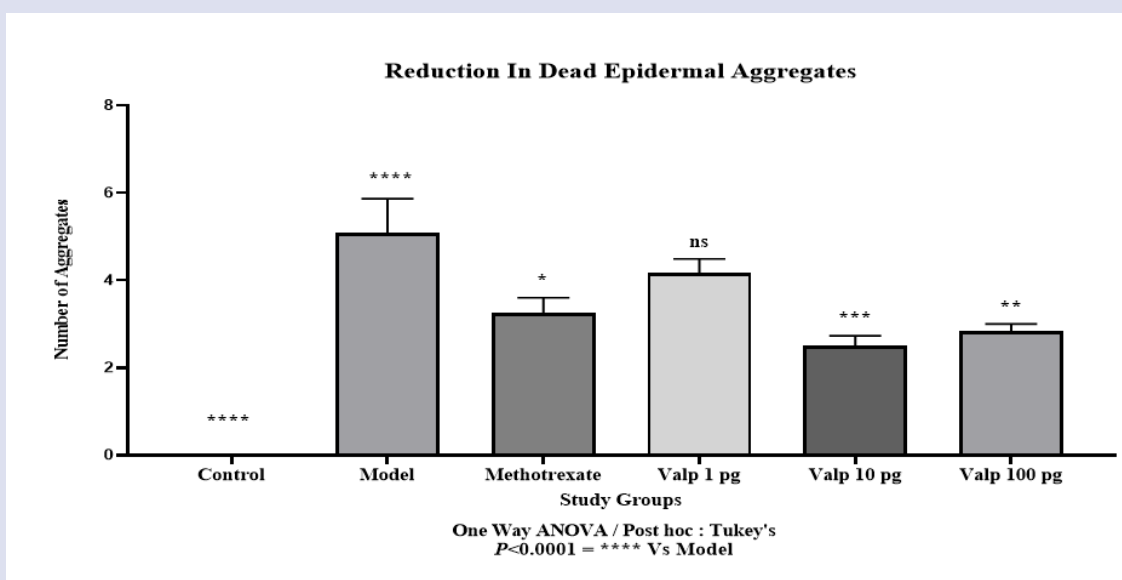


Figure 9: Reduction in dead epidermal aggregates.

Therefore, a dose dependent rescue was observed across Valp treated group.

Assay 2: Erythema – distribution of redness in pixel intensity

The distribution of redness in pixel intensity correlation is deliberated in this section and the table 6 shows the Erythema- Distribution of redness in pixel intensity.

Figure 10 represents measure of distribution of redness in pixel intensity in the extremities such as caudal and pectoral fins. The mean of control was compared with the mean of model. Control and model exhibited significant difference in the distribution of red pixel intensity. Model exhibited highest distribution of red pixel conforming presence of erythema. Mean of model was compared to mean of Methotrexate treated group. Methotrexate treated group showed significant reduction in the distribution of red pixel indicating mild rescue. Mean of model was compared to Valp treated groups. Valp treated group exhibited a dose dependent rescue across various dilution. Valp at 1 pg showed moderate decrease in distribution of red pixel intensity indicating moderate rescue. Valp at 10 pg and 100 pg showed gradual decrease in distribution of red pixel intensity indicating moderate rescue.

Assay 3: Induration - measures of thickness of aggregates

The correlation between the study groups and thickness of the aggregates are discussed in the following and the table 7 shows the measure of thickness of aggregates.

Figure 11 represents measure of thickness of aggregates where mean model was compared with mean of control. Control did not show presence of aggregates whereas model displayed higher number of aggregates with average thickness of 0.22 mm. Mean of model was compared to Methotrexate treated group. Methotrexate treated group exhibited significant reduction in thickness of the aggregates indicating mild rescue. Mean of model was compared to Valp treated groups across various dilution. Valp at 1 pg, 10 pg and 100 pg did not show any reduction in thickness of aggregates. Therefore, no rescue was observed across the treated dilutions.

Assay 4: Desquamation - measures of descaling on the epidermis

The measure of descaling on the epidermis are shown in followings; Zebrafish Larvae image at 40X magnification; (a) Control, (b) Model, (c) Methotrexate, (d) Valp 1 pg, (e) Valp 10 pg, (f) Valp 100 pg is shown

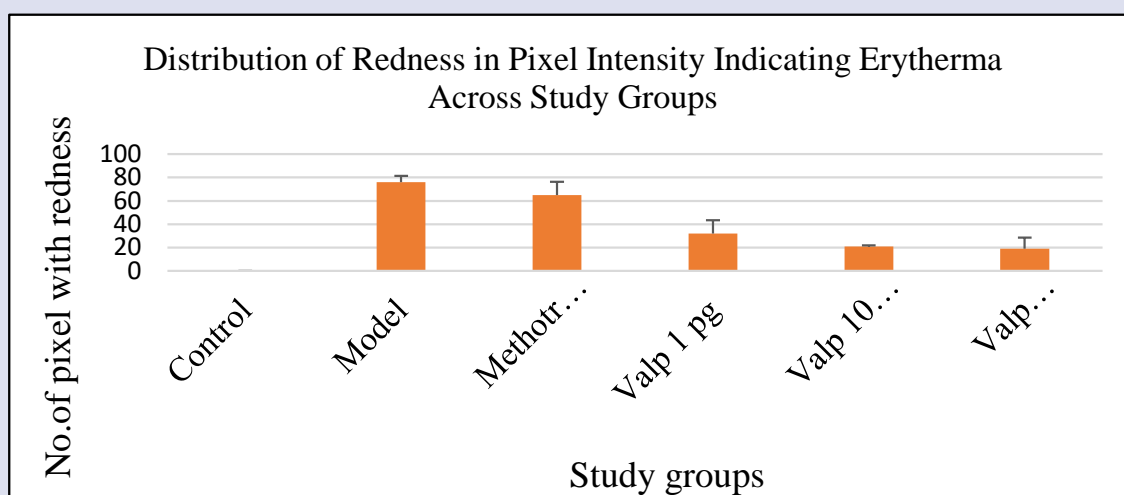


Figure 10: Erythema – distribution of redness in pixel intensity.

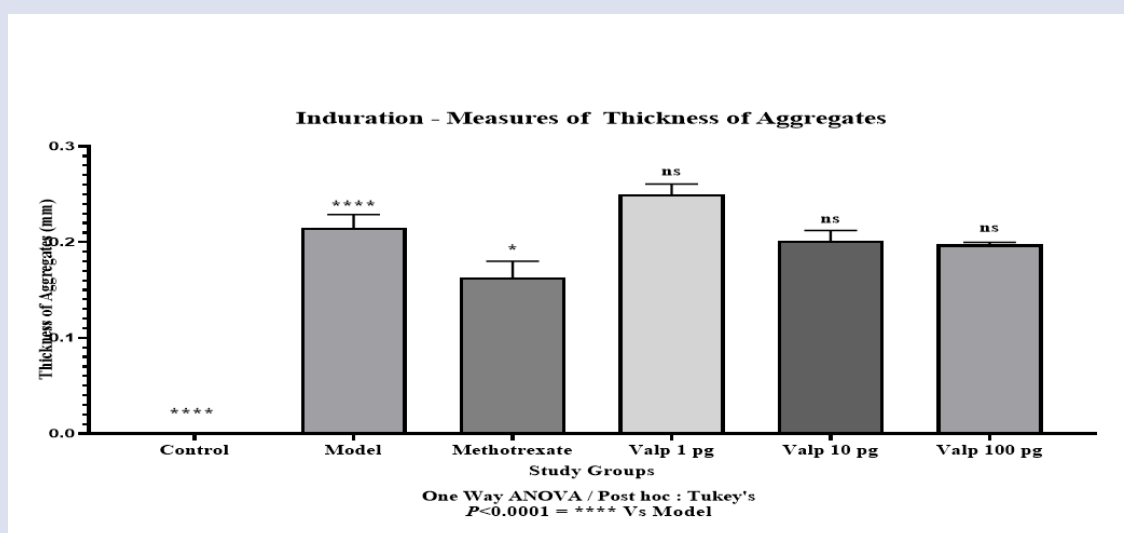


Figure 11: Induration – measure of thickness of aggregates.

in figure 12. Table 1 shows the Desquamation – Measure of Area of Desquamation.

Figure 13 represents measure of area of desquamation where mean of control was compared to model. Control and model showed significant difference in area of desquamation. Compared to control, model displayed discontinuous extremities (caudal and pectoral fin) indicating loss of epithelial cells confirming desquamation as represented in the figure 4 with graphical line Mean of model was compared to of Methotrexate treated group. Methotrexate treated group displayed a significant decline in area of desquamation indicating moderate rescue. The mean of model was compared to Valp treated groups. Valp at 10 pg and 100 pg exhibited gradual decline in area of desquamation indicating moderate rescue. Whereas Valp at 1 pg showed mild reduction in area of desquamation indicating mild rescue. Valp exhibited dose dependent rescue across the dilutions.

Assay 5: Cell proliferation assay: expression profile of tnp1 gene by semi quantitative RT PCR

The cell proliferation assay is shown in assay 5, it denotes the expression profile of tnp1 gene by semi quantitative RT PCR. Table 9 shows the

DNA repair gene expression profile. Gel Image from gel electrophoresis of the PCR product is shown in figure 14.

Lane 1- 100 bp DNA ladder, Lane 2 - 18s rRNA of Control, Lane 3 - 18s rRNA of Model, Lane 4 - 18s rRNA of Methotrexate, Lane 5 - 18s rRNA of Valp 1 pg, Lane 6 - 18s rRNA of Valp 10 pg, Lane 7 - 18s rRNA of Valp 100 pg, Lane 8 – tnp1 of Control, Lane 9 – tnp1 of Model, Lane 10 – tnp1 of Methotrexate, Lane 11 – tnp1 of Valp 1 pg, Lane 12 – tnp1 of Valp 10 pg, Lane 13 – tnp1 of Valp 100.

Figure 15 represents fold change in gene expression of tnp1 gene where control and model exhibited significant difference in fold change. Control exhibited 1.39 fold changes whereas in model tnp1 gene was downregulated with -2.53-fold change. The gene expression of tnp1 gene was found to be downregulated in Methotrexate treated group with -4.38-fold change and in Valp treated group across all the dilutions. The downregulation of tnp1 gene is associated with the increase in cell proliferation in psoriasis condition in zebrafish larvae. Therefore, Valp treated group across various dilutions showed moderate rescue in decreasing cell proliferation and did not completely rescue in decreasing cell proliferation.

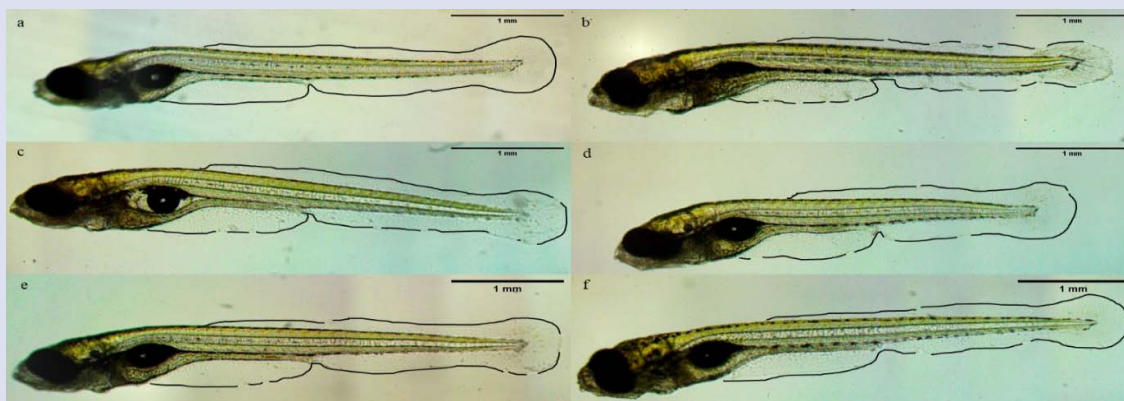


Figure 12: Zebrafish larvae image at 40X magnification; (a) Control, (b) Model, (c) Methotrexate, (d) Valp 1 pg, (e) Valp 10 pg, (f) Valp 100 pg.

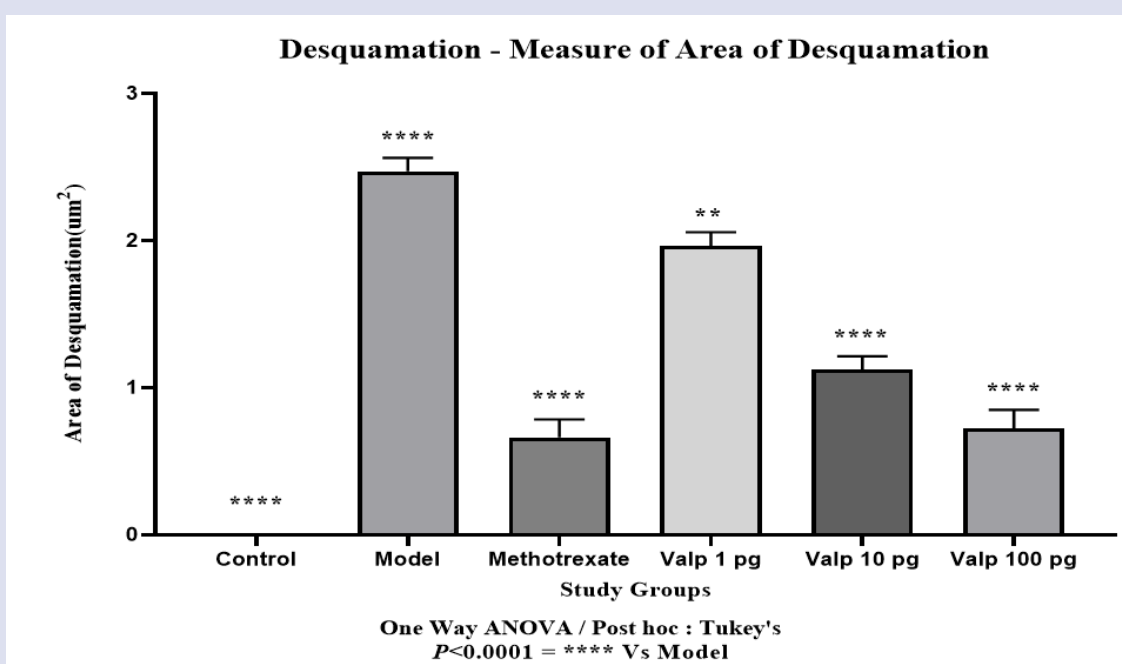


Figure 13: Represents desquamation - measures of area of desquamation.



Figure 14: Gel image from gel electrophoresis of the PCR product.

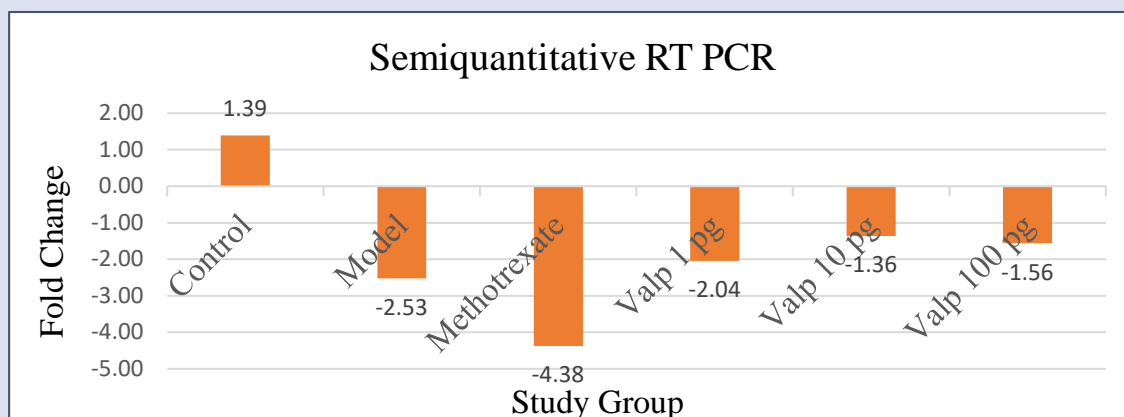


Figure 15: Represents expression profile of tnip1 gene.

Table 7: Measure of thickness of aggregates.

Study Groups	Thickness of the Aggregates (mm)	SD
Control	0.00	0.00
Model	0.22	0.05
Methotrexate	0.16	0.06
Valp 1 pg	0.25	0.04
Valp 10 pg	0.20	0.04
Valp 100 pg	0.20	0.01

Table 8: Desquamation – measure of area of desquamation.

Study Groups	Area of Desquamation (um ²)	SD
Control	0.00	0.00
Model	2.47	0.23
Methotrexate	0.66	0.35
Valp 1 pg	1.97	0.31
Valp 10 pg	1.12	0.28
Valp 100 pg	0.72	0.43

Table 9: DNA repair gene expression profile.

Study Groups	Fold Change
Control	1.39
Model	-2.53
Methotrexate	-4.38
Valp 1 pg	-2.04
Valp 10 pg	-1.36
Valp 100 pg	-1.56

Table 10: Adopted PASI score.

Study Groups	Severity Score	Percentage Severity	Severity
Control	0.0000	0	Normal
Model	0.0220	100	Severe
Methotrexate	0.0113	50	Severe
Valp 1 pg	0.0060	27	Severe
Valp 10 pg	0.0058	26	Severe
Valp 100 pg	0.0010	5	Mild

Assay 5: Adopted PASI score

The adopted PASI score is deliberated in the following table 10. The correlation is performed with respect to the study groups and severity score.

Figure 16 represents percentage severity where the mean of model was compared with control. Control and model showed significant difference in percentage severity. Model exhibited maximum PASI score indicating the severity of psoriasis symptoms. Mean of model was compared to methotrexate treated group. Methotrexate treated group exhibited 50 percent severity with decline in PASI Score indicating no rescue across the psoriasis symptoms. Mean of model was compared to Valp treated groups. Valp treated groups exhibited dose dependent reduction of PASI score over model ranging from 27 to 5 percent. Valp at 1 pg and 10 pg showed significant decrease in PASI score with that of the model with 26 and 27 percent severity respectively, indicating no rescue across the psoriasis symptoms. Whereas Valp at 100 pg showed a significant decrease in PASI score with 5 percent score indicating moderate rescue of the model.

Genotoxicity

Expression profile of mgmt gene by semi quantitative RT PCR

The evaluation and the result obtained in the Genotoxicity are discussed in this section. Table 11 shows the DNA repair gene expression profile. Gel Image from gel electrophoresis of the PCR product is shown in figure 17.

Lane 1- 100 bp DNA ladder, Lane 2 - 18s rRNA of Control, Lane 3 - 18s rRNA of Model, Lane 4 - 18s rRNA of Methotrexate, Lane 5 - 18s rRNA of Valp 1 pg, Lane 6 - 18s rRNA of Valp 10 pg, Lane 7 - 18s rRNA of Valp 100 pg, Lane 8 – mgmt of Control, Lane 9 – mgmt of Model, Lane 10 – mgmt of Methotrexate, Lane 11 - mgmt of Valp 1 pg, Lane 12 - mgmt of Valp 10 pg, Lane 13 - mgmt of Valp 100

Figure 18 represents fold change in gene expression of mgmt gene where control and model exhibited significant difference in fold change. The fold change in gene expression of mgmt gene was higher in control by 1.1-fold whereas model showed 0.90-fold change. The gene expression of mgmt gene was found to be downregulated in methotrexate and Valp at 1 pg treated groups. Whereas gene expression of mgmt gene in Valp 10 pg and 100 pg treated group showed marginal increment with

Table 11: DNA repair gene expression profile.

Study Groups	Fold Change
Control	1.15
Model	0.90
Methotrexate	-1.13
Valp 1 pg	-1.53
Valp 10 pg	0.96
Valp 100 pg	0.77

Table 12: Survival rate.

Study Groups	Survival Percentage %
Control	100
Model	83
Methotrexate	83
Valp 1 pg	83
Valp 10 pg	92
Valp 100 pg	100

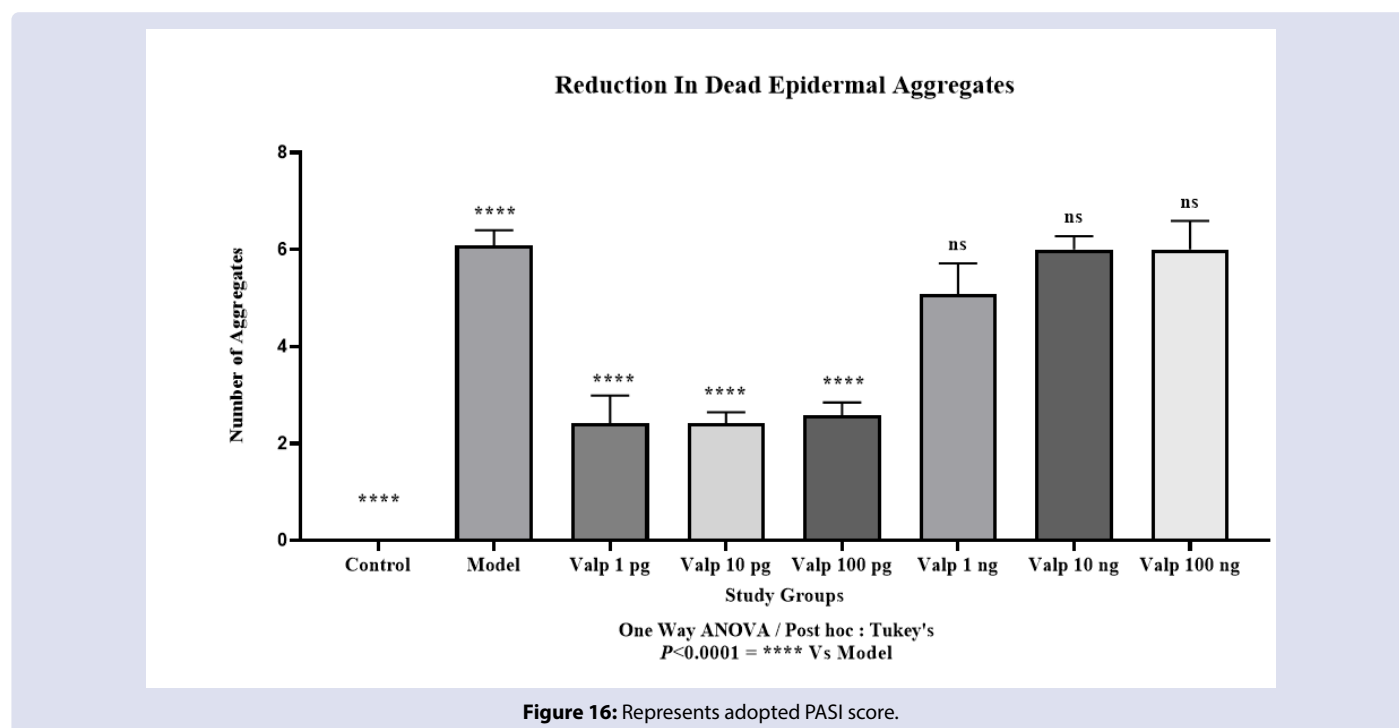


Figure 16: Represents adopted PASI score.

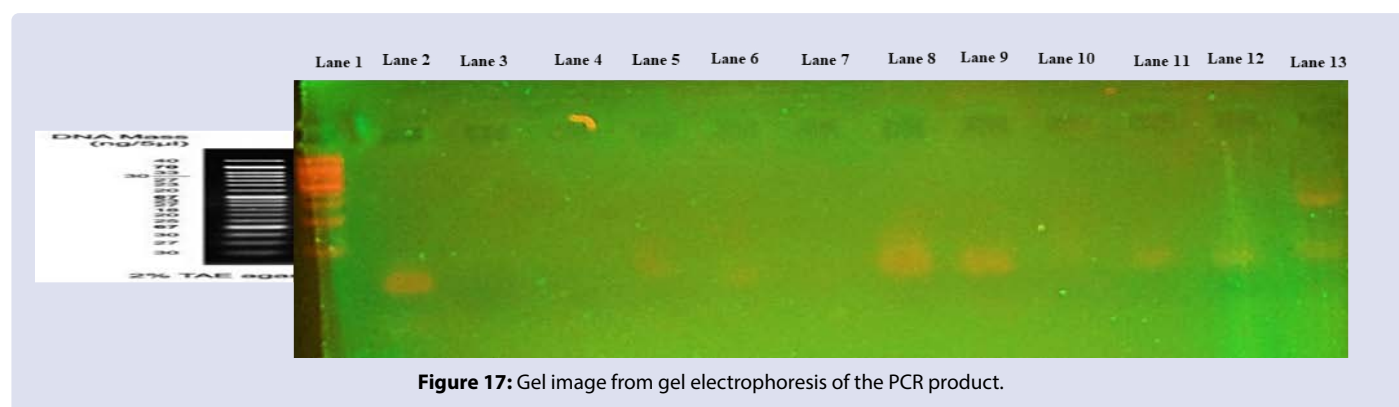


Figure 17: Gel image from gel electrophoresis of the PCR product.

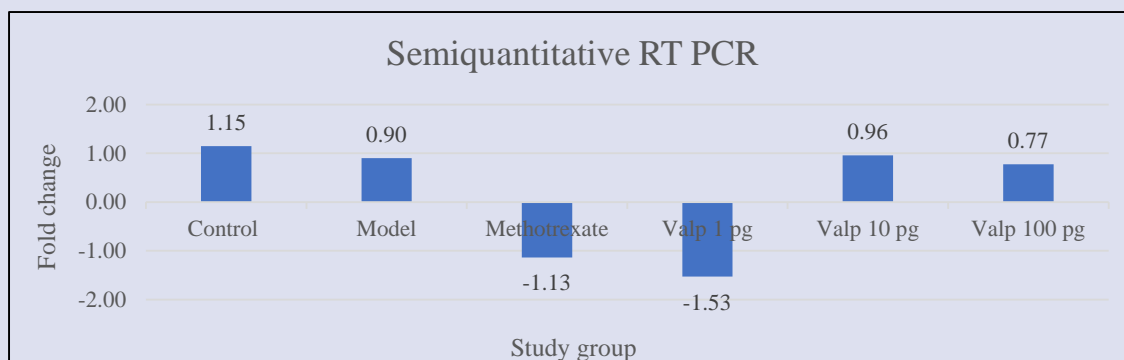


Figure 18: Represents expression profile of mgmt gene.

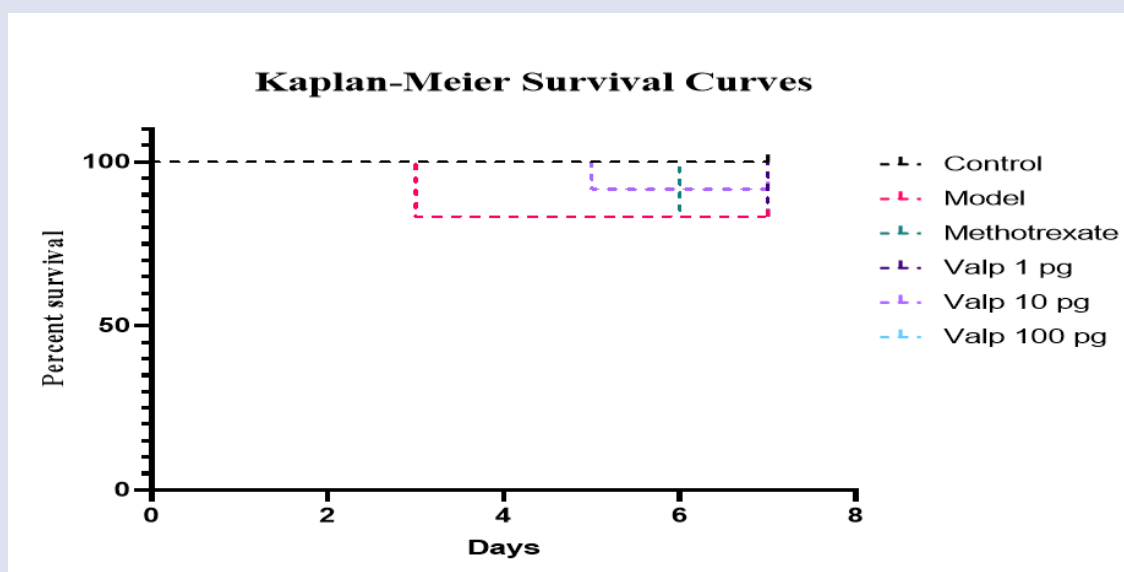


Figure 19: Represents Kaplan-Meier survival curve.

0.96 and 0.77-fold respectively. Increment in mgmt gene expression level is associated with DNA repair occurring in the zebrafish larvae. Therefore, no genotoxicity was observed at 100 pg.

Kaplan-Meier survival curve – drug screening and genotoxicity

The Kaplan-Meier survival curve for drug screening and genotoxicity results are deliberated in this section. Table 12 resulted the survival rate in percentage for each study group.

Figure 19 represents the Kaplan Meier survival curve of the larvae for drug screening and genotoxicity. The WT showed a 100% survival rate and no mortality. Whereas model marked 83% survival with 2 larvae mortality on day 3. Methotrexate treated group showed 83% survival with mortality spread across day 6 throughout the study period. The mortality of Valp treated group at 1 pg showed 83% survival with highest mortality event recorded on day 7. Valp at 10 pg showed 92% survival with one mortality record on day 7. and Valp 100 pg, showed 100% survival rate with no mortality throughout the study period. Methotrexate and Valp at 1 pg is observed to be the least survival group among all the groups in the study. Overall Valp at 100 pg showed better survival with no mortality.

DISCUSSION

In terms of the awareness of the safe use of natural products and the increasing demand from the consumers side who prefer to switch

to natural components from synthetic additives to treat the regular discomfort in health, requires an appropriate balance between the therapeutic and toxicological effects of the natural/herbal products.⁵⁵ Any beneficial medicinal plant must therefore be evaluated for its possible mutagenic and genotoxic effects before being used in treatment. According to research reports, *V. pachynema* contains a wealth of bioactive chemicals with maximum anti-oxidant activity⁵⁶ but there is no available literature with regard to pre-clinical genotoxicity studies of its crude extract. In light of this, we carried out a series of *in vivo* genetic toxicology tests and drug toxicity assays to investigate the marine algal extract's potential for mutagenic and genotoxic effects.

The present study highlights for the first time the toxicity profile, anti-inflammatory capacities and the therapeutic efficacy of the marine seaweed *V. pachynema*. In this study, anti-inflammatory activity and the drug toxicity were observed in the marine algae *Valoniopsis pachynema* using methanolic extract. Previous studies have shown that *Valoniopsis pachynema* high anti-oxidant activity. The anti-inflammatory impact of the formulated methanol extract from *V. pachynema* have been examined by the inhibitory characteristics of albumin-denaturation.

The anti-inflammatory effect of the methanol extraction from *V. pachynema* has been explored by the albumin denaturation inhibition. As an alternative to traditional animal testing, *in vivo* studies on zebrafish embryos were conducted to determine the toxicity and therapeutic effects of the crude compound. The zebra fish has gained popularity as a model for biomedical research and is used in industrial

fields and toxicology. Zebrafish can be utilised to explore biological targets and behavioural patterns due to its genetic engineering. Due to their relative convenience and ease of handling, the use of embryos in place of traditional animal testing is particularly receiving interest.⁵⁷

CONCLUSION

According to the latest findings, *V. pachynema* contains higher levels of biochemicals, vitamins, and minerals, and secondary metabolites of this green marine algae has shown optimistic anti-inflammatory properties. The secondary metabolites also contain several active functional groups that exhibit vast chemical expansions. In the present study, the efficacy, therapeutic efficacy, and genotoxicity of the methanol crude extraction of the green seaweed *V. pachynema* at various concentration was determined by recapitulating the pathophysiology of Skin inflammation in Zebrafish larvae. The compounds were checked across various clinical end points. In efficacy study, Valp at 1 pg, 10 pg, 100 pg was observed to have efficacy and were advanced for evaluation of therapeutic efficacy and genotoxicity. In investigation of therapeutic efficacy, zebrafish larvae were treated with Valp at 1 pg, 10 pg and 100 pg and were monitored across various clinical end points. Overall Valp at 100 pg exhibited moderate rescue in reduction of dead epidermal aggregates, erythema, desquamation and exhibited decrease in PASI score indicating moderate rescue across the symptoms of psoriasis with 100% survival rate. However, no rescue was observed across the treated dilutions in induration and decrease in cell proliferation.

Although, Methotrexate exhibited moderate rescue in reduction of dead epidermal aggregates and desquamation only a mild rescue was observed in erythema and induration. On whole methotrexate displayed marginal reduction in PASI score indicating 50% severity. In evaluation of genotoxicity, the gene expression of mgmt gene was observed to be in control level at Valp 100 pg treated group confirming no genotoxicity. The proposed research work is a clearly a different approach as it has attempted to evaluate the potential mutagenic and genotoxic impacts of methanol extraction of the *V. pachynema* marine-algae with in-vitro anti-inflammatory activity and in-vivo genotoxicity assay. The outcomes obtained has clearly confirmed the analyzed extract does not cause any mutagenic or genotoxic damage to the living cells under the examined conditions. Thus, it can be concluded that the test extract is safe and can be employed in nutraceutical, chemical and pharmaceutical industries related application. As suggested previously, it was also observed that the algae could be used as effective antioxidants for the prevention of diseases.

ACKNOWLEDGEMENT

None

CONFLICTS OF INTEREST

The authors declare that they have no conflicts of interest.

AUTHORS CONTRIBUTIONS

All authors contributed to the study conception and design. All authors read and approved the final manuscript.

FUNDING

There is no funding for this study.

REFERENCES

1. Murthy AS, Leslie K. Autoinflammatory skin disease: a review of concepts and applications to general dermatology. *Dermatology*. 2016;232(5):534-40.
2. Gordon S. The role of the macrophage in immune regulation. *Res Immunol*. 1998;149(7-8):685-8.
3. Gautam R, Jachak SM, Saklani A. Anti-inflammatory effect of *Ajuga bracteosa* Wall Ex Benth. mediated through cyclooxygenase (COX) inhibition. *J Ethnopharmacol*. 2011;133(2):928-30.
4. Vo T-S, Ngo D-H, Van Ta Q, Wijesekara I, Kong C-S, Kim S-K. Protective effect of chitin oligosaccharides against lipopolysaccharide-induced inflammatory response in BV-2 microglia. *Cell Immunol*. 2012;277(1-2):14-21.
5. Bejarano JJR, Valdecantos WC. Psoriasis as autoinflammatory disease. *Dermatol Clin*. 2013;31(3):445-60.
6. Hou R, Li J, Niu X, Liu R, Chang W, Zhao X, et al. Stem cells in psoriasis. *J Dermatol Sci*. 2017;86(3):181-6.
7. Lebwohl M. Psoriasis. *Ann Intern Med*. 2018;168(7).
8. Raposo I, Torres T. Palmoplantar psoriasis and palmoplantar pustulosis: current treatment and future prospects. *Am J Clin Dermatol*. 2016;17(4):349-58.
9. Renton C. Diagnosis and treatment of adults with scalp psoriasis. *Nurs Standard*. 2014;28(26).
10. Syed ZU, Khachemoune A. Inverse psoriasis. *Am J Clin Dermatol*. 2011;12(2):143-6.
11. Dutta S, Chawla S, Kumar S. Psoriasis: A review of existing therapies and recent advances in treatment. *Differentiation*. 2018;2:10.
12. Menter MA, Armstrong AW, Gordon KB, Wu JJ. Common and not-so-common comorbidities of psoriasis. *Semin Cutan Med Surg*. 2018;37(2S):48-51.
13. Helmick CG, Sacks JJ, Gelfand JM, Bebo Jr B, Lee-Han H, Baird T, et al. Psoriasis and psoriatic arthritis: a public health agenda. *Am J Prev Med*. 2013;44(4):424-6.
14. Jin D-Q, Lim CS, Sung J-Y, Choi HG, Ha I, Han J-S. Ulva conglobata, a marine algae, has neuroprotective and anti-inflammatory effects in murine hippocampal and microglial cells. *Neurosci letters*. 2006;402(1-2):154-8.
15. Kang S-M, Kim K-N, Lee S-H, Ahn G, Cha S-H, Kim A-D, et al. Anti-inflammatory activity of polysaccharide purified from AMG-assistant extract of *Ecklonia cava* in LPS-stimulated RAW 264.7 macrophages. *Carbohydrate Polym*. 2011;85(1):80-5.
16. Wang H-MD, Chen C-C, Huynh P, Chang J-S. Exploring the potential of using algae in cosmetics. *Biores Technol*. 2015;184:355-62.
17. Sanjeeva KKA, Kim E-A, Son K-T, Jeon Y-J. Bioactive properties and potentials cosmeceutical applications of phlorotannins isolated from brown seaweeds: A review. *J Photochem Photobiol B: Biol*. 2016;162:100-5.
18. Admassu H, Gasmalla MAA, Yang R, Zhao W. Bioactive peptides derived from seaweed protein and their health benefits: antihypertensive, antioxidant, and antidiabetic properties. *J Food Sci*. 2018;83(1):6-16.
19. Kaliaperumal N, Ramalingam J, Kalimuthu S, Ezhilvalavan R. Seasonal changes in growth, biochemical constituents and phycocolloid of some marine algae of Mandapam coast. *Seaweed Res Utilisation*. 2002;24(1):73-7.
20. Ji NK, Kumar R, Patel K, Viyol S, Bhoi R. Nutrient composition and calorific value of some seaweeds from bet dwarka, west coast of Gujarat, India. *Our Nature*. 2009;7(1):18-25.
21. Jha B, Reddy C, Thakur MC, Rao MU. Seaweeds of India: the diversity and distribution of seaweeds of Gujarat coast: Springer Science & Business Media; 2009.
22. Kaliaperumal N, Kalimuthu S. Seaweed potential and its exploitation in India. *Seaweed Research and Utilisation*. 1997;19(1&2):33-40.
23. Dhinakaran DI, Geetha P, Rajalakshmi J. Antioxidant activities of marine algae *Valoniopsis pachynema* and *Sargassum swartzii* from the south east coast of India. *Int J Fisheries Aquatic Stud*. 2015;3(2):426-30.

24. Selva Kumar R, Chandrasekaran V. Valoniopsis pachynema extract as a green inhibitor for corrosion of brass in 0.1 N phosphoric acid solution. Metallurgical Materials Transactions B. 2016;47(2):891-8.
25. Sanandiya ND, Mukesh C, Prasad K, Siddhanta A. Evaluation of cellulose of Valoniopsis pachynema (Martens) Børgesen for its applications in paper making. J Appl Phycol. 2017;29(3):1657-62.
26. Lakshmikandan M, Murugesan A. Enhancement of growth and biohydrogen production potential of Chlorella vulgaris MSU-AGM 14 by utilizing seaweed aqueous extract of Valoniopsis pachynema. Renewable Energy. 2016;96:390-9.
27. Lakshmikandan M, Murugesan A. Chlorella vulgaris MSU-AGM 14, a fresh water microalgal strain-growth and photobiological hydrogen production in acid hydrolysate of seaweed Valoniopsis pachynema. Int J Hydrogen Energy. 2016;41(32):13986-92.
28. Mahomoodally MF, Bibi Sadeer N, Zengin G, Cziáky Z, Jekő J, Diuzheva A, et al. In vitro enzyme inhibitory properties, secondary metabolite profiles and multivariate analysis of five seaweeds. Marine Drugs. 2020;18(4):198.
29. Breton J, Le Clère K, Daniel C, Sauty M, Nakab L, Chassat T, et al. Chronic ingestion of cadmium and lead alters the bioavailability of essential and heavy metals, gene expression pathways and genotoxicity in mouse intestine. Arch Toxicol. 2013;87(10):1787-95.
30. Rivera N, Rojas M, Zepeda A, Malagón F, Arán VJ, Marrero-Ponce Y, et al. In vivo genotoxicity and cytotoxicity assessment of a novel quinoxalinone with trichomonacide activity. J Appl Toxicol. 2013;33(12):1493-9.
31. De Sibio MT, Luvizotto RAM, Olimpio RMC, Correia CR, Marino J, de Oliveira M, et al. A comparative genotoxicity study of a supra-physiological dose of triiodothyronine (T3) in obese rats subjected to either calorie-restricted diet or hyperthyroidism. PLoS One. 2013;8(2):e56913.
32. Wu H-J, Liu C, Duan W-X, Xu S-C, He M-D, Chen C-H, et al. Melatonin ameliorates bisphenol A-induced DNA damage in the germ cells of adult male rats. Mutation Research/Genetic Toxicol Env Mutagenesis. 2013;752(1-2):57-67.
33. Chakravarthy S, Sadagopan S, Nair A, Sukumaran S. Zebrafish as an. Vivo; 2014.
34. Barbazuk WB, Korf I, Kadavi C, Heyen J, Tate S, Wun E, et al. The syntenic relationship of the zebrafish and human genomes. Genome research. 2000;10(9):1351-8.
35. Kimmel CB, Ballard WW, Kimmel SR, Ullmann B, Schilling TF. Stages of embryonic development of the zebrafish. Dev Dynamics. 1995;203(3):253-310.
36. Rihel J, Prober DA, Schier AF. Monitoring sleep and arousal in zebrafish. Methods in cell biology. 100: Elsevier; 2010;281-94.
37. Taylor KL, Grant NJ, Temperley ND, Patton EE. Small molecule screening in zebrafish: an in vivo approach to identifying new chemical tools and drug leads. Cell Commun Signaling. 2010;8(1):1-14.
38. Wittmann C, Reischl M, Shah AH, Mikut R, Liebel U, Grabher C. Facilitating drug discovery: an automated high-content inflammation assay in zebrafish. JoVE. 2012(65):e4203.
39. Lessman CA. The developing zebrafish (*Danio rerio*): A vertebrate model for high-throughput screening of chemical libraries. Birth Defects Research Part C: Embryo Today: Reviews. 2011;93(3):268-80.
40. Tsang M. Zebrafish: a tool for chemical screens. Birth Defects Research Part C: Embryo Today: Reviews. 2010;90(3):185-92.
41. Love DR, Pichler FB, Dodd A, Copp BR, Greenwood DR. Technology for high-throughput screens: the present and future using zebrafish. Curr Opin Biotechnol. 2004;15(6):564-71.
42. Amsterdam A, Lin S, Hopkins N. The Aequorea victoria green fluorescent protein can be used as a reporter in live zebrafish embryos. Dev Biol. 1995;171(1):123-9.
43. Finley KR, Davidson AE, Ekker SC. Three-color imaging using fluorescent proteins in living zebrafish embryos. Biotechniques. 2001;31(1):66-72.
44. Keller PJ, Schmidt AD, Wittbrodt J, Stelzer EH. Reconstruction of zebrafish early embryonic development by scanned light sheet microscopy. Sci. 2008;322(5904):1065-9.
45. Niell CM, Meyer MP, Smith SJ. In vivo imaging of synapse formation on a growing dendritic arbor. Nature Neurosci. 2004;7(3):254-60.
46. Williams PR, Morgan JL, Kerschensteiner D, Wong RO. In vivo imaging of zebrafish retina. Cold Spring Harbor Protocols. 2013;2013(1):pdb. prot072652.
47. Mizushima Y, Kobayashi M. Interaction of anti-inflammatory drugs with serum proteins, especially with some biologically active proteins. J Pharm Pharmacol. 1968;20(3):169-73.
48. Kaur S, Syed Ali M, Anuradha V, Suganya V, Ashashalini A, Bhuvana P. In vitro anti-inflammatory activity of mangrove plant Rhizophora mucronata Lam. (Malpighiales: Rhizophoraceae). Brazilian J Biol Sci. 2018;5(10):417-26.
49. Solnica-Krezel L, Stemple DL, Mountcastle-Shah E, Rangini Z, Neuhauss S, Malicki J, et al. Mutations affecting cell fates and cellular rearrangements during gastrulation in zebrafish. Development. 1996;123(1):67-80.
50. Webb AE, Driever W, Kimelman D. Psoriasis regulates epidermal development in zebrafish. Dev Dynam. 2008;237(4):1153-64.
51. IV JPM, Berghmans S, Zahrieh D, Neuberger DS, Kanki JP, Look AT. Zebrafish sperm cryopreservation with N, N-dimethylacetamide. Biotechniques. 2003;35(5):956-68.
52. Chen Y, Yan H, Song Z, Chen F, Wang H, Niu J, et al. Downregulation of TNIP1 expression leads to increased proliferation of human keratinocytes and severer psoriasis-like conditions in an imiquimod-induced mouse model of dermatitis. PloS One. 2015;10(6):e0127957.
53. Chomczynski P, Sacchi N. Single-step method of RNA isolation by acid guanidinium thiocyanate-phenol-chloroform extraction. Analytical biochemistry. 1987;162(1):156-9.
54. Driever W, Solnica-Krezel L, Schier A, Neuhauss S, Malicki J, Stemple D, et al. A genetic screen for mutations affecting embryogenesis in zebrafish. Development. 1996;123(1):37-46.
55. Bello A, Padmanabhan S, Thangamalai R, Lakshmanan K, Nagarajan K. Evaluation of genotoxic effects of methanolic extract of brown seaweed Stoechospermum marginatum. J Phytopharmacol. 2019;8(5):226-31.
56. Tc Dca. Evaluation of Bioactive Substances And Biochemical Composition of Valoniopsis pachynema (Martens) Boerger AND Stoechospermum marginatum (Ag.) Kutz. Int J Creative Res Thoughts (IJCRT). 2022;10(5):445-52.
57. Ha Y, Kim Y, Choi J, Hwang I, Ko J-Y, Jeon HK, et al. Evaluation of cytotoxicity, genotoxicity, and zebrafish embryo toxicity of mixtures containing Hyssopus officinalis, Morus alba, Engraulis japonicus, and 27 other extracts for cosmetic safety assessment. Mol Cell Toxicol. 2021;17(2):221-32.

Cite this article: Bhuvaneshwari J, Vasan PT. Bio-Evaluation, *In-Vitro* and *In-Vivo* Anti-Inflammatory Activity, Therapeutic Efficacy, and Genotoxicity of the Potentials of the Green Seaweed *Valoniopsis Pachynema* using Zebra Fish Larvae (*Danio Rerio*) as an Animal Model. Pharmacogn J. 2022;14(6)Suppl: 1037-1053.